CHEMICAL ENGINEERING TRANSACTIONS
VOL. 120, 2025
A publication of AIDIC
The Italian Association of Chemical Engineering
Online at www.cetjournal.it
Guest Editors: Bing Shen How, Viknesh Andiappan, Denny K.S. Ng, Hon Loong Lam, Petar S. Varbanov

**ISBN** 979-12-81206-21-2; **ISSN** 2283-9216
DOI: 10.3303/CET25120031

# Operational Analysis of Solar Thermal Storage System Using COMSOL Multiphysics for Industrial Applications

Cristobal R. Díaz-de-León[a], Jazmín Martínez-Sánchez[a], Juan-Carlos Baltazar[b], Guillermo Martínez-Rodríguez[a,*]

[a]Department of Chemical Engineering, University of Guanajuato, Guanajuato 36050, Mexico
[b]Texas A&M University, College Station 3581, U.S.A.
guimarod@ugto.mx

The storage system guarantees the continuous supply of the heat load, at target temperature, to an industrial process. This system represents 30 % of the total cost of solar thermal installation. A thermo-hydraulic characterization was performed in a 60 $m^3$ storage system with recirculation using the software COMSOL and the 2D finite element method, maximizing the use of solar energy and the time in which the target temperature is reached and minimizing the volume required to supply the heat load to the process. A pasteurization process was selected with a heat load of 880 kW and target temperature of 75 °C. A 2D configuration was used to design the storage tank and the separator baffle with a porosity of 40 %. A 60 $m^3$ storage tank loaded with water at ambient temperature was simulated in COMSOL Multiphysics software. The solar collector network was designed considering winter irradiance levels in Guanajuato city, Mexico. Compared with storage system designs reported in the literature, the period of time with a temperature equal to or greater than the target temperature is 47.37 % higher, the maximum storage temperature increased by 5.5 %, and the volume required to supply the heat load decreased by 9.8 %.The system guarantees the full supply of the heat load by eliminating $CO_2$ emissions and minimizing storage system cost.

## 1. Introduction

The industrial sector is one of the largest energy consumers worldwide. In 2022, 166 EJ were consumed, corresponding to 37 % of the global consumption (IEA, 2023); in 2023, it increased by 2 % (IEA, 2024). Energy production in the industrial sector is mainly carried out with fossil fuels; in 2022, 65 % was by this method (IEA, 2023). In 2024, renewable energies represented the greatest growth in global demand, with a total of 13.9 EJ, or 38 % of the total (IEA, 2025). By 2024, the total number of installed solar heat for industrial processes (SHIP plants) was 1,209, with an area of 1.359 B $m^2$ and a capacity of 951 MW (SHC, 2024). In Mexico, by the end of 2022, there was a total capacity of solar thermal systems for the industrial sector of 13.4 MW and an installed area of 34,868.87 $m^2$ (Ituna-Yudonago et al., 2025). Thermal energy storage systems (TES) are an indispensable component of industrial solar thermal applications, ensuring a continuous supply to the process despite intermittent solar resources. The main forms of thermal energy storage for industrial processes are chemical (CES), electrochemical (ECES), sensible heat (SHTES) and latent heat (LHTES) thermal storage systems (Desai et al., 2021). TES technologies have been implemented in various applications, such as district heating, cold chains, space heating, and concentrated solar power plants (CSP). However, their penetration in the industrial sector has been very low, accounting for around 1 % of total installed storage capacity (Nichols, 2024). The total installed thermal storage capacity is estimated at 234 GWh in 2019 and is expected to increase to 800 GWh by 2030 (Statista, 2024). The costs of storage systems depend on the installed capacity and supply time, as well as parameters such as the storage medium, tank and support structure, having an approximate cost of 20, 67 and 16 USD/kWh respectively (U. S. Department of Energy, 2022) for a 100 MW steam production plant and 8 h of operation.

There are several studies that analysed the impact of storage systems, type of materials and configurations in solar thermal applications. Li et al. (2024) studied different storage technologies for a concentrator plant, which

Paper Received: 01 May 2025; Revised: 28 August 2025; Accepted: 23 September 2025
Please cite this article as: Díaz-de-León C.R., Martínez-Sánchez J., Baltazar J.-C., Martínez-Rodríguez G., 2025, Operational Analysis of Solar Thermal Storage System Using COMSOL Multiphysics for Industrial Applications, Chemical Engineering Transactions, 120, 181-186 DOI:10.3303/CET25120031

were a molten salt tank, a packed bed with solid material and a phase change material. The average efficiencies of the systems were 26, 25.5 and 24.5 respectively. The packed bed technology allows a cost reduction of 21.2 and 42.3 %, as well as a storage volume of 83 and 63.8 % for the system with phase change material and solid respectively. Mathew and Thangavel (2021) designed and evaluated a novel thermal storage system incorporated into an agricultural product dehydrator. The storage system contained Therminol 55 as the working fluid, irradiance conditions were evaluated from June to August, the maximum temperature obtained was 133 °C, the maximum thermal efficiency obtained was 30 % and the drying time was reduced by 2 h with a payback of 2.6 y.

An important part of studying storage systems is carrying out experimental analyses of the thermal and hydraulic behaviour that occurs inside the tank to validate theoretical studies. However, due to the complexity of assembling the system and the high costs associated with materials, measuring instruments and working conditions, some researchers have implemented numerical modelling or performed analyses through simulations to predict the loading and unloading processes of storage systems (He et al., 2022) to design and optimise solar thermal systems. Zhang et al. (2023) performed an analysis using COMSOL Multiphysics modelling on a thermochemical storage system assisted with a PVT collector and a heat exchanger for heating (building space heating) under Nottingham environmental conditions. The storage charge and discharge were simulated, selecting a fine mesh for the simulations and performing a parametric analysis of operation, a system efficiency of 56 % was determined, the highest thermal efficiency obtained was for a reactor bed length of 0.5 m. Salvestroni et al. (2021) carried out a modelling in COMSOL Multiphysics for the storage of a solar district heating system in Italy. Through a parametric analysis of the system and a finer mesh, an optimal configuration was reached with a storage volume of 3800 $m^3$, a solar absorption system of 1,000 $m^2$ and a solar fraction of 0.44. Xue et al. (2022) carried out experimental analysis and modelling using IDA ICE and COMSOL Multiphysics for borehole thermal energy storage systems up to 310 m deep in Otaniemi, Finland. The system mesh was triangular with a total of $1.3x10^6$ elements. Simulation results showed very small temperature variations compared to those obtained experimentally. A simplified IDA ICE arrangement can reduce simulation time by up to 72 %. Méndez and Bicer (2021) modelled a storage system considering different solid materials as a working medium, located in the bottom section of a solar chimney using COMSOL Multiphysics, the solar chimney has a turbine coupled for power production. A mesh sensitivity analysis (or grid independence study) was performed using fine, normal, and coarse meshes, comparing pressure, temperature, and wind velocities values. The results showed a maximum variation in results of 1 % between meshes, the average power production was 27.46 kW at 72 °C for phase change materials, while for solid materials up to 31.49 kW of power at 79 °C and an annual energy efficiency of 0.122 % were obtained.

Using the 2D finite element method and COMSOL Multiphysics software, through thermohydraulic characterization, the total cost of a solar thermal storage system was minimized by 12.5 % and the time during which the temperature was equal to or greater than the target temperature was maximized. This was done for an industrial-scale case study, a milk pasteurization process. No solar thermal energy storage system has been reported in the literature that describes the actual operation of the system as described in this article. The storage system operates with recirculation and always removes available solar energy, increasing the system's thermal performance, minimizing system costs, and ensuring the thermal load is maintained at the target temperature.

## 2. Using COMSOL Multiphysics software to minimize the cost of a solar thermal storage system

Solar thermal storage systems are necessary devices to ensure the operation of industrial processes. The main components of solar thermal installation are the solar collector network, the solar thermal storage system, and the control system. Solar thermal installation design considers the variability of solar resources, critical irradiance levels, and consecutive days with irradiance levels below critical levels. The main objective is to ensure the continuous supply of the heat duty at the target temperature with the lowest storage system cost. The thermos-economic evaluation of a recirculating storage system exemplifies the actual operation of a collector network and a storage system. The solar collector network and the solar thermal storage system were designed with the methodology proposed by Martínez-Rodríguez et al. (2019) based on daily point irradiance during the winter period. The lowest irradiance levels are recorded during the winter; therefore, the storage system design guarantees the supply of the heat duty throughout the year. The environmental conditions data was obtained from the meteorological station of the University of Guanajuato for the year 2024. The geographical location is 21.03 latitude and -101.27 longitude. The average environmental conditions during the year are irradiance 503.41 $W/m^2$, ambient temperature 21.2 °C, wind velocity 2.87 m/s and relative humidity 40 %. The daylight period during the winter season is from 7:30 to 18:15 h having a total of 10.75 h of sunlight. The

storage system temperature is 85 °C, with a temperature gradient of 10 °C between the hot and cold streams. Figure 1 shows an overview diagram of the proposed system.
For the COMSOL Multiphysics simulation, the solar thermal storage system was built in a 2D configuration. The selected modules were fluid flow and heat transfer, and the physical interfaces used were laminar flow and liquid heat transfer to simulate the water flow conditions within the storage system and the temperature change of the feedwater from the solar collector network, respectively.

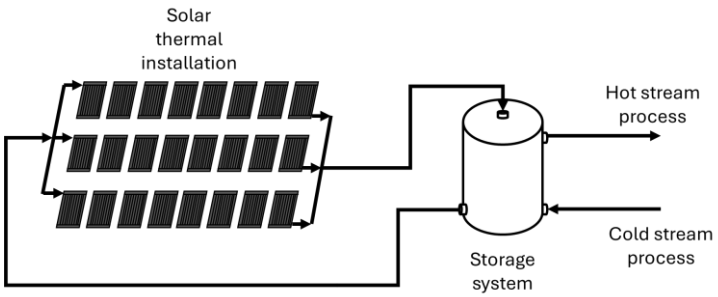


*Figure 1: Solar thermal energy storage tank powered by a network of solar collectors.*

The storage tank is proposed to have a perforated separator baffle implemented, which reduces mixing effects and heat losses. The baffle was selected based on the geometries available on the international market (Kapwell, 2024). The COMSOL geometric model of the baffled storage tank was created using the interface's Sketch mode. To build the model, object primitives were added to the model sketch. These primitives are the basic geometric shapes in COMSOL, such as rectangles, squares, and circles. The geometric figures available in the components section were used, and the geometric dimensions of height, diameter, tank thickness, inlet and outlet pipe diameters, and the separating baffle were specified. Using the Union tool, the shapes added to the sketch were joined into a single component to obtain the model of the study system. Next, the tank material and working fluid were defined. For the simulation, the physical phenomena associated with heat transfer and momentum transfer were established, and the initial conditions of the recirculating solar thermal energy storage system were defined, for example, the inlet temperature to the storage tank, which varies over time, and the inlet flow temperature to the tank, which is constant over time. The mesh in the system model was constructed based on the system geometry to solve the equations associated with the transport phenomena. A temporal model was used to determine the behaviour of the working fluid storage during operating hours. The results allowed for the visualisation of temperature profiles, velocity profiles, and the thermal and hydraulic behaviour of the working fluid inside the tank. The working fluid used is water, and the tank is made of carbon steel and has no insulation.
The storage tank was selected based on the volume of hot water required for an industrial process. Table 1 shows the geometric characteristics of the tank available on the international market (We-Mac Tanks, 2024).

*Table 1: Storage tank dimensions.*

| Volume | Height | Diameter | Thickness | Diameter of inlet and outlet pipes |
|---|---|---|---|---|
| 60 $m^3$ | 6 m | 3.6 m | 2 cm | 10 cm |

The loading process in the storage tank was studied considering water recirculation. The baffle opening area is 40 % (Lou et al., 2020) and is located 3 m from the base of the tank. The hot water inlet is in the centre of the upper cover and the outlet is in the lower left corner, 10 cm from the base. A uniform distribution of perforations across the cross-section in the center of the tank was also proposed, each with a diameter of 5 cm, obtained from the opening area and the tank diameter. The geometry of the baffle impacts the water velocity gradient at the top of the tank, where the greatest degree of mixing occurs. At the bottom of the tank, water velocities along the vertical and horizontal axes are more homogeneous, and mixing is less. With less mixing, the water temperature inside the tank is more uniform, and there is a lower gradient between the feed from the collector network and the stored water. The tank inlet temperature is a variable function of operating time, obtained from daytime irradiance conditions. The mesh was refined, increasing its resolution and number of elements, which allows for results very close to the analytical solution. However, the computational effort required to obtain the results also increases considerably. Meshes with various resolutions were considered, termed coarser, coarse, and normal, with a total of 20,978, 25,898, and 29,248 domain elements, respectively. A sensitivity analysis of

the mesh was performed to ensure the accuracy of the results; since there was no significant variation between the coarse and normal meshes, the normal mesh (29,248 elements) was chosen for the study. Figure 2 shows the different meshes selected and the resolution of each.

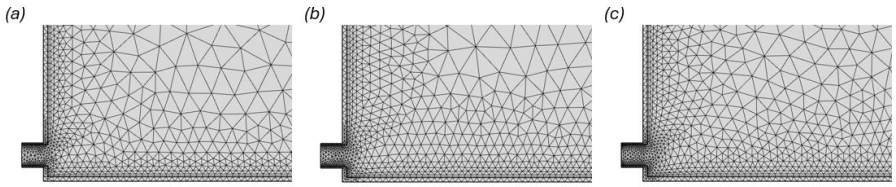


*Figure 2: Comparison of the meshes: (a) Coarser, (b) Coarse, (c) Normal*

Figure 3 represents the outlet water temperature of a finite number of solar collectors connected in series, which is a function of irradiance. The maximum outlet temperature is reached at solar noon. The adjustment of the different points (temperature, time) is performed using least-squares polynomial regression. The points that make up the parabolic temperature profile are those with a temperature equal to or greater than the target temperature (90 °C). The operating period is from 7:30 to 14:30 h. The storage tank is initially filled with water at 20 °C, and the mass flow rate of water in the feed and outlet was 0.75 kg/s.

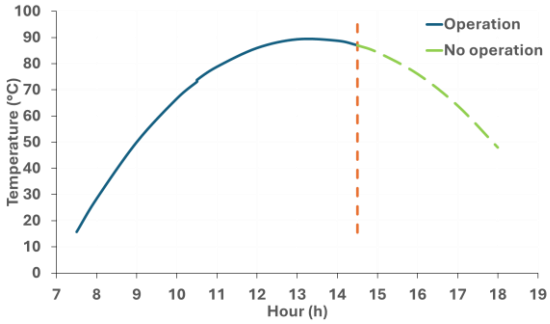


*Figure 3: Temperature profile during operating hours.*

### 2.1 Case study: Pasteurization in a dairy industry

The pasteurization process consists of sudden heating to 75 °C for a period of 15 to 20 s (Lott et al., 2023). Pasteurization eliminates pathogens in the milk and preserves the food. The process operates for 5 h per day (4,400 kWh/d) and requires a heat load of 880 kW, at a target temperature of 75 °C.
The solar thermal installation is designed to supply the entire heat load $\dot{Q} = 880\ kW$, at target temperature. The amount of hot water required by the pasteurization process at 84 °C is determined using Eq(1).

$$Q_{tot} = m_{H_2O} C_{p_{H_2O}} \Delta T \quad (1)$$

where $m_{H_2O}$ is the mass of water required for the pasteurization process, kg; $C_{p_{H_2O}}$ is the heat capacity of water, kJ/kg°C; $\Delta T$ is the temperature difference between the stored water (84 °C) and the ambient temperature (20 °C). The volume of the storage tank was obtained using Eq(2) (Yang et al., 2014). Water density: 1,000 kg/m$^3$.

$$V = \frac{Q_{HTST\ tot}}{\rho_{H_2O} C_{p_{H_2O}} \Delta T} \quad (2)$$

The investment cost of the storage tank is calculated by a ratio of the reported price for commercial equipment to the storage volume (Sateña, 2022). The cost function $C = A * \frac{V}{15.8}\ , USD$; where $A$ = 39,856.4. Installation, operation, maintenance costs, taxes, and subsidies are not considered.

## 3. Results

The feedwater temperature profile obtained for the irradiance conditions of a winter day is a quadratic function ($T = at^2 + bt + c$) that relates the outlet water temperature of the solar collectors and the operating time of the

solar thermal system. At 10:30 h, a water temperature of 80 °C is reached. The values of the constants in the profile are $= -2.5259$, $b = 64.613$ and $c = -326.84$ for the time interval from 7:30 to 10:30 h and $a = -1.9318$, $b = 51.609$ and $c = -255.11$ for the interval from 10:30 to 14:30 h. The simulated solar thermal system was in operation from 7:30 to 14:30 h, during which 60 m$^3$ of hot water at 90 °C was obtained. Figure 4 shows the temperature distribution profiles and the velocity field inside the tank at 14:30 h.

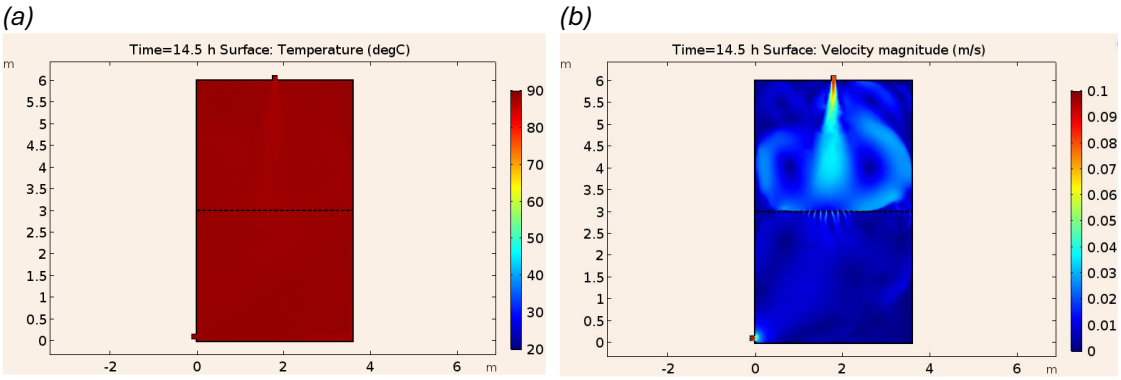


*Figure 4: Temperature of (a) water in the tank; and (b) internal velocity at 14:30 h.*

The temperature distribution profile indicates that water inside the tank is at a homogeneous temperature of 90 °C. The velocity field profile shows that at the bottom of the baffle the velocity magnitudes are small compared to the tank inlet, tank outlet and the upper part to the separator baffle, indicating that the degree of mixing inside the tank is small. Table 2 shows the comparison between the obtained results and the results reported by Martínez-Rodríguez et al. (2019). Conventionally, the solar thermal system is operated during the operating period in which the highest outlet temperature is (4.75 h), guaranteeing the heat load at the target temperature of 85 °C. By recirculating the water from 7:30 to 14:30 h, 7 h is the time in which a temperature equal to or greater than the target temperature is reached (47.37 % higher compared to Martínez-Rodríguez et al., 2019). The solar thermal system outlet temperature of 90 °C reduces the volume of water required by the process (60 to 54.11 m$^3$). To determine the volume of a hot water storage tank, it is assumed that it can only be filled up to 80 % of the total volume. An 80 m$^3$ tank is required for 60 m$^3$ of water, and a 70 m$^3$ tank is required for 54.11 m$^3$. Consequently, the storage tank cost savings are 12.5 %.

*Table 2: Comparison of results for process storage with reported results by Martínez-Rodríguez et al. (2019).*

| Parameter | Reported in literature | Proposal in this paper |
|---|---|---|
| Volume of water | 60 m$^3$ | 54.11 m$^3$ |
| Volume of tank | 80 m$^3$ | 70 m$^3$ |
| Temperature | 85 °C | 90 °C |
| Operating time | 4.75 h | 7 h |
| Storage tank cost | USD$ 201,805 | USD$ 176,579 |

The maximum temperature reached in the proposed storage system was 5.55 % higher than that reported by Martínez-Rodríguez et al. (2019). This increase in temperature reduces the volume required by the process by 9.8 %. This results in a hot water surplus of 5.89 m$^3$. The storage cost is reduced by 12.5 %.

## 4. Conclusions

Using COMSOL Multiphysics simulations, this study characterized the momentum and heat transfer occurring in a recirculating solar thermal energy storage tank connected to a solar collector network. The water in the tank increased its temperature with increasing irradiance over the course of a day. The selected baffle ensured a homogeneous temperature throughout the tank during operation.

The proposed storage system clearly represents how a tank operates in a real-life situation. The volume required by the industrial process is continuously recirculated when conditions allow for temperature increases based on irradiance. This reduces the cost (12.5 %), increases the time (7 h) to reach the target temperature required by the process, and the maximum temperature reached of 90 °C is higher than reported in the literature.

Considering the velocity and temperature profiles, it is concluded that there are no stagnation zones in the tank.

**References**

Desai F., Jenne S.P., Muthukumar P., Rahman M.M., 2021, Thermochemical energy storage system for cooling and process heating applications: A review. Energy Conversion and Management, 229, 113617.

He X., Qiu J., Wang W., Hou Y., Ayyub M., Shuai Y., 2022, A review on numerical simulation optimization design and applications of packed-bed latent thermal energy storage system with spherical capsules. Journal of Energy Storage, 51, 104555.

IEA, 2023, International Energy Agency, <www.iea.org/energy-system/industry>, accessed 20.03.2025.

IEA, 2024, International Energy Agency, <www.iea.org/reports/world-energy-outlook-2024>, accessed 20.03.2025.

IEA, 2025, International Energy Agency, <www.iea.org/reports/global-energy-review-2025>, accessed 20.03.2025.

Ituna-Yudonago J.F., García-Valladares O., Ortíz-Rodríguez N.M., Ibarra-Bahena J., Galindo-Luna Y.R., 2025, Applications of solar thermal technologies in Mexican industries for heating processes and their contribution against global warming: An overview. Solar Energy, 291, 113395.

Kapwell, 2024, Perforated Baffle Plates, <kapwell.co.uk/products/separator-internals/perforated-baffle-plates/>, accessed 25.05.2025.

Li M.J., Li M.J., Jiang R., Du S., Li X.Y., 2024, Study on the dynamic characteristics of a concentrated solar power plant with the supercritical CO2 Brayton cycle coupled with different thermal energy storage methods. Energy, 288, 129628.

Lou W., Fan Y., Luo L., 2020, Single-tank thermal energy storage systems for concentrated solar power: Flow distribution optimization for the thermocline evolution management. Journal of Energy Storage, 32, 101749.

Lott T.T., Wiedmann M., Martin N.H., 2023, Shelf-life storage temperature has considerably larger effect than high-temperature, short-time pasteurization temperature on the growth of spore-forming bacteria in fluid milk. Journal of Dairy Science, 106 (6), 3838-3855.

Martínez-Rodríguez G., Fuentes-Silva A.L., Lizárraga-Morazán J.R., Picón-Núñez M., 2019, Incorporating the Concept of Flexible Operation in the Design of Solar Collector Fields for Industrial Applications. Energies,12, 570.

Mathew A.A., Thangavel V., 2021, A novel thermal energy storage integrated evacuated tube heat pipe solar dryer for agricultural products: Performance and economic evaluation. Renewable Energy, 179, 1674-1693.

Méndez C., Bicer Y., 2021, Comparison of the influence of solid and phase change materials as a thermal storage medium of the performance of a solar chimney. Energy Science & Engineering, 9, 1274-1288.

Nichols C., Thermal Energy Storage Technologies for Industrial Heating Application, 2024, IDTechEx, < www.idtechex.com/en/research-article/thermal-energy-storage-technologies-for-industrial-heating-application/31120>, accessed 20.04.2025.

Salvestroni, M., Pierucci, G., Pourreza, A., Fagioli, F., Taddei, F., Messeri, M., De-Lucia, M., 2021, Design of a solar district heating system with seasonal storage in Italy, Applied Thermal Engineering, 197,117438.

SATEÑA Pressure Vessels & Engineering, 2022, Sateña S. A. de C. V., <www.satena.com.mx/index.html>, accessed 26.05.2025.

SCH Solar Heat World Wide, 2024, Solar Heating & Cooling Programe-International Energy Agency, <www.iea-shc.org/solar-heat-worldwide>, accessed 20.04.2025.

Statista Installed capacity of thermal energy storage worldwide in 2019, with a forecast for 2030, Statista, < www.statista.com/statistics/1307219/thermal-energy-storage-capacity-global/>, accessed 21.04.2025.

U.S.D.E. 2022 Grid Energy Storage Technology Cost and Performance Assessment, 2022, U. S. Department of Energy, <www.energy.gov/sites/default/files/2022-09/2022%20Grid%20Energy%20Storage%20Technology%20Cost%20and%20Performance%20Assessment.pdf>, accessed 20.04.2025.

We-Man Tanks, 2024, <https://wemactanks.com/tank-charts/>, accessed 30.12.2024.

Xue T., Jokisalo J., Kosonen R., Vuolle M., Marongiu F., Vallin S., Leppâharju N., Arola T., 2022, Experimental evaluation of IDA ICE and COMSOL models for an asymmetric borehole thermal energy storage field in Nordic climate. Applied Thermal Engineering, 217, 119261.

Yang P., Liu L., Du J., Li J., Meng Q., 2014, Heat exchanger network synthesis for batch processes by involving heat storages with cost targets. Applied Thermal Engineering, 70, 1276-1282.

Zhang Y., Hu M., Chen Z., Su Y., Riffat S., 2023, Modelling analysis of solar-driven thermochemical energy storage unit combined with heat recovery. Renewable Energy, 206, 722-737.